Available online www.jocpr.com

Journal of Chemical and Pharmaceutical Research, 2013, 5(5):72-88

Research Article

ISSN : 0975-7384
CODEN(USA) : JCPRC5

Conformational stability, vibrational spectral studies, HOMO-LUMO and NBO analyses of 2-bromo-1-Indanol based on quantum chemical calculations

V. Balachandran[a*], V. Karpagam[b] and G. Santhi[c]

[a]*Research Department of Physics, A A Government Arts College, Musiri, India*
[b]*Department of Physics, Srinivasan Polytechnic College, Perambalur, India*
[c]*PG Department of Physics, Government Arts College, Karur, India*

ABSTRACT

Indanol is most stable molecule it's stabilized by internal hydrogen bonding, which exists between the hydroxyl hydrogen and the π–cloud of the benzene ring. A comprehensive ab initio calculation using the DFT/ 6-31+G (d) level theory showed that 2-bromo1-Indanol can exist in eight possible conformations, which can interchange through the OH group on the five-membered ring. Density functional theory calculations were used to predict the vibrational frequencies and to help in normal mode assignments. The spectral intensities indicate that, at 90°C, 82% of the molecules exist in its most stable form with the intramolecular hydrogen bonding. Furthermore, a natural bond orbitial analysis was performed describing each hydrogen bond as donor-accepter interaction. The Fourier transform infrared spectra (4000–400 cm^{-1}) and the Fourier transform Raman spectra (3500–100 cm^{-1}) of the title molecule in the solid space have been recorded. The calculated HOMO and LUMO energies show that charge transfer occurs within the molecule. The calculated ESP contour map shows the electrophilic and nucleophilic region of the molecule.

Keywords: 2-bromo1-indanol, FT-IR, FT-Raman, DFT, HF, Thermodynamic function.

INTRODUCTION

1-Indanone may be considered as the central nucleus of a vast set of compounds with a wide assortment of biomedical applications [1]. Of these, indandiols stand out due to the increasing demand for optically pure compounds with biological activity [2]. Also, a relatively new application of 1-indanone derivatives is related to the treatment of HIV infection as an important new class of protease inhibitors. In particular, indinavir sulphate (CRIXIVAN Merck and Co., Inc.) contains five chiral centres' that must be of a specific orientation for the molecule to have the desired therapeutic effect. The key intermediate in the synthesis of CRIXIVAN is cis-(1s, 2R) - 1-amino-2-indanol [(–)-CA1)], an indene derivative that contributes two chiral centres to indinavir sulphate [3].

The detailed vibrational analyses for 1-indanone were given by Bardet *etal* [4] made use of IR and Raman in the region of 4000 -100 cm^{-1} recorded in solution and assuming Cs point group symmetry. The practical application of vibrational spectroscopy is the combined use of experimental techniques and theoretical calculations to achieve a reliable vibrational assignment. Ab initio and DFT calculations have greatly enhanced the accuracy of this methodology not only by predicting the vibrational wavenumbers, but also their intensities.

In the present paper, we turn our attention to 2-bromo-1-Indanol, which is special interest due to its possibility of intramalecular hydrogen bonding between the OH group and the benzene ring.

The scaled quantum mechanical force field [SQM] methodology [5-8] was applied along with a refinement of the scale factors in order to fit the experiment frequencies of 2-bromo 1-indanol with the harmonic frequencies. Our aim in the present work is a thorough analysis of the intermolecular interactions and how it is affect the vibrational spectra. The natural bond orbital analysis (NBO) calculations are useful to confirm the charge transfer properties of the title molecule. The molecule Electrostatic potential map shows various sites for electrophilic, and nucleophilic region.

EXPERIMENTAL SECTION

Experimental

The pure solid sample of 2BI was obtained from Lancaster Chemical Company, UK, and used for the spectral measurements without further purification. The room temperature Fourier transform infra red spectrum of the title compound was measured in the region 4000-400 cm^{-1}, at a resolution of ± 1 cm^{-1} , using a BRUKER IFS 66V FT-IR Spectrometer, equipped with an MCT detector, a KBr beam splitter and a globar source. The FT- Raman spectrum was recorded on the same instrument with FRA 106 Raman accessories in the region 3500-100 cm^{-1}. The 1064nm Nd:YAG Laser was used as excitation source, and the Laser power was set to 200mW.

Computational method

Quantum chemical calculation were used for 2BI to carry out the optimized geometry and vibrational wavenumbers with the Gaussian 09W program [9] using the B3LYP and HF functional [10, 11] supplemented with standard 6-31+G (d) basis set. For the plots of simulated IR and Raman spectra pure Lorentz an band shapes were used with a band width (FWHW) of 10 cm^{-1}. The vibrational modes were assigned by means of visual inspection using GAUSS VIEW program [12], the analysis for the vibrational modes of 2BI is presented in some detail in order to better describe the basis for the assignments, from these basic theory of Raman scattering. Raman activities (S_i) calculated by Gaussian 09w program has been converted to relative Raman intensities (I_i) using the following relationship

$$I_i = \frac{f\left(\upsilon_0 - \upsilon_i\right)^4 S_i}{\upsilon_i\left[1-\exp\left(\frac{-hc\upsilon_i}{kT}\right)\right]}$$

where υ_o is the exciting wavenumber (cm^{-1} units) υ_i is the vibrational wavenumber of the i^{th} normal mode, h, c and k are universal constant and f is a suitably chosen common normalization factor for all peak intensities.

Natural bond orbital analysis(NBO) was also performed by the Gaussian 09W program at the B3LYP level of theory analysis transforms the canonical delocalized Hartree-Fork (HF) Molecular orbital's (MO) in to localized MOs that are closely tied to chemical bonding concepts. This process involves sequential transformation of non-orthogonal Atomic obital's (AOs) to the sets of Natural atomic orbital's (NAOs), Natural hybrid orbital's (NHOs), Natural bond orbital's (NBOs). The localized basis sets are completely describes the wave functions in the most economic method, as electron density and other properties that are described by the minimum amount of filled NBOs describe the hypothetical, strictly localized Lewis structure. The interaction between filled and anti-bonding (or Rydberg) orbital's represent the deviation of the molecule from the Lewis structure and be used as the measure of delocalization. This non-covalent bonding anti-bonding charge transfer interactions can be quantitatively described in terms of the second order perturbation interaction energy ($E^{(2)}$) [13-16]. This energy represents the estimate of the off-diagonal NBO Fock matrix elements. It can be deduced from the second-order perturbation approach [17] as follows

$$E^{(2)}\Delta E_{ij} = q_i \frac{F(i,j)^2}{\varepsilon_j - \varepsilon_i}$$

where q_i is the i^{th} donor orbital occupancy, ε_j, ε_i the diagonal elements (orbital energies) and $F(i, j)$ the off-diagonal NBO Fock matrix element.

RESULTS AND DISCUSSION

Structural description

In order to find the most optimized geometry, the energies were carried out for 2BI, using B3LYP/6-31+G (d) and HF/6-31+G (d) methods and basis set for various possible conformers. The computationally predicted various possible conformers are shown in Fig.1. The total energies obtained for these conformers were listed in Table 1. It is clear from the Table1, the structure optimizations have shown that the conformer of Fig. 1 (C5) have produced the global minimum energy. The optimized molecular structure with the numbering of atoms of the title compound is shown in Fig. 2. The most optimized structural parameters were also calculated by B3LYP and HF was depicted in Table 2. The optimized geometrical parameters were used to compute the vibrational frequencies of the stable conformer (C5) of 2BI at the B3LYP/and HF level of theory

For this purpose, the full sets of standard internal coordinates (containing-redundancies) are defined as given in Table 3. From these a non-redundant set of local symmetry coordinates was constructed by suitable linear combination of internal coordinates following the recommendations of Fogarasi and Pulay [18] and they are presented in Table 4. The theoretically calculated force field was transformed to this later set of vibrational coordinates and was used in all subsequent calculations.

Table 1 Total energies of different conformations of 2-bromo 1-Indanol calculated at the HF/ 6–31+G (d) and B3LYP / 6–31+G (d) level of theory

S no	Total energy		Energy difference	
	HF/ 6–31+G (d)	B3LYP/ 6–31+G (d)	HF/ 6–31+G (d)	B3LYP/ 6–31+G (d)
1	–2990.58646566	–2995.11823727	0.1600202	0.13810126
2	–2990.58131780	–2995.11271829	0.16516808	0.14362024
3	–2990.60671116	–2995.13434292	0.1397747	0.12199561
4	–2990.60385114	–2995. 13123868	0.14263472	0.12509985
5	–2990.74648586*	–2995.25633853*	0	0
6	–2990.74312521	–2995.25215144	0.00336065	0.00418709
7	–2990.72361409	–2995.23675992	0.02287177	0.01957861
8	–2990.72667054	–2995.23746951	0.01981532	0.01886902

**Global minimum energy*

Table 2 Definition of internal co-ordinates of 2-bromo 1-Indanol

Sno	Symbol	Type	Definition
1-10	R	CC	C1–C2, C2–C3, C9–C3, C9–C4, C4–C5, C5–C6, C6–C7, C7–C8, C8–C9, C8–C1
11-18	T	CH	C1–H10, C2–H14, C3–H15, C3–H16, C4–H17, C5–H18, C6–H19, C7–H20
19	P	CO	C1–O11
20	Q	CBr	C2–Br13
21	S	OH	O11–H12
22-30	B	bCC	C1–C2–C3, C2–C3–C9, C9–C3–C4, C3–C4–C5, C4–C5–C6, C5–C6–C7, C7–C8–C9, C7–C8–C1, C9–C3–C2,
31-46	α	bCH	C9–C1–H10,C2–C1–H10,C7–C6–H19,C8–C7–H19,C1–C2–H14,C3–C2–H14,C9–C3–H15,C2–C3–H15,C9–C3–H16,C2–C3–H16,C9–C5–H17,C5–C4–H17, C6–C5–H18,C4–C5–H18,C6–C7–H20,C8–C7–H20
47-48	α	bCO	C8–C1–O11,C2–C1–O11
49-50	ρ	bCBr	C1–C2–Br13, C3–C2–Br13
51	μ	bCOH	C1–O11–H12
52	γσπ	bHOH	H10–O11–H12
53		HCBr	H14–C2–Br13
54		Ring	C1–C2–C3–C9,C2–C3–C9–C4,C9–C3–C4–C5,C3–C4–C5–C6,C4–C5–C6–C7,C5–C6–C7–C8,C7–C8–C9–C4,C7–C8–C1–C2,C8–C1–C2–C3
63-70		ωCH	C8–C1–C2–H14,C1–C2–C3–H15,C1–C2–C3–H16,C1–C8–C7–H20,C3–C9–C4–H17,C4–C9–C3–H16,C4–C5–C6–H19,C8–C7–C6–H19
71		ωCO	C9–C8–C1–O11
72, 73		ωOH	C8–C1–O11–H12, C2–C1–O11–H12
74		ωBr	C1–C2–C3–Br13
75		ωHCOH	H10–C1–O11–H12
76		ωHCH	H10–C1–C2–H14
77		ωHCBr	H10–C1–C2–Br13

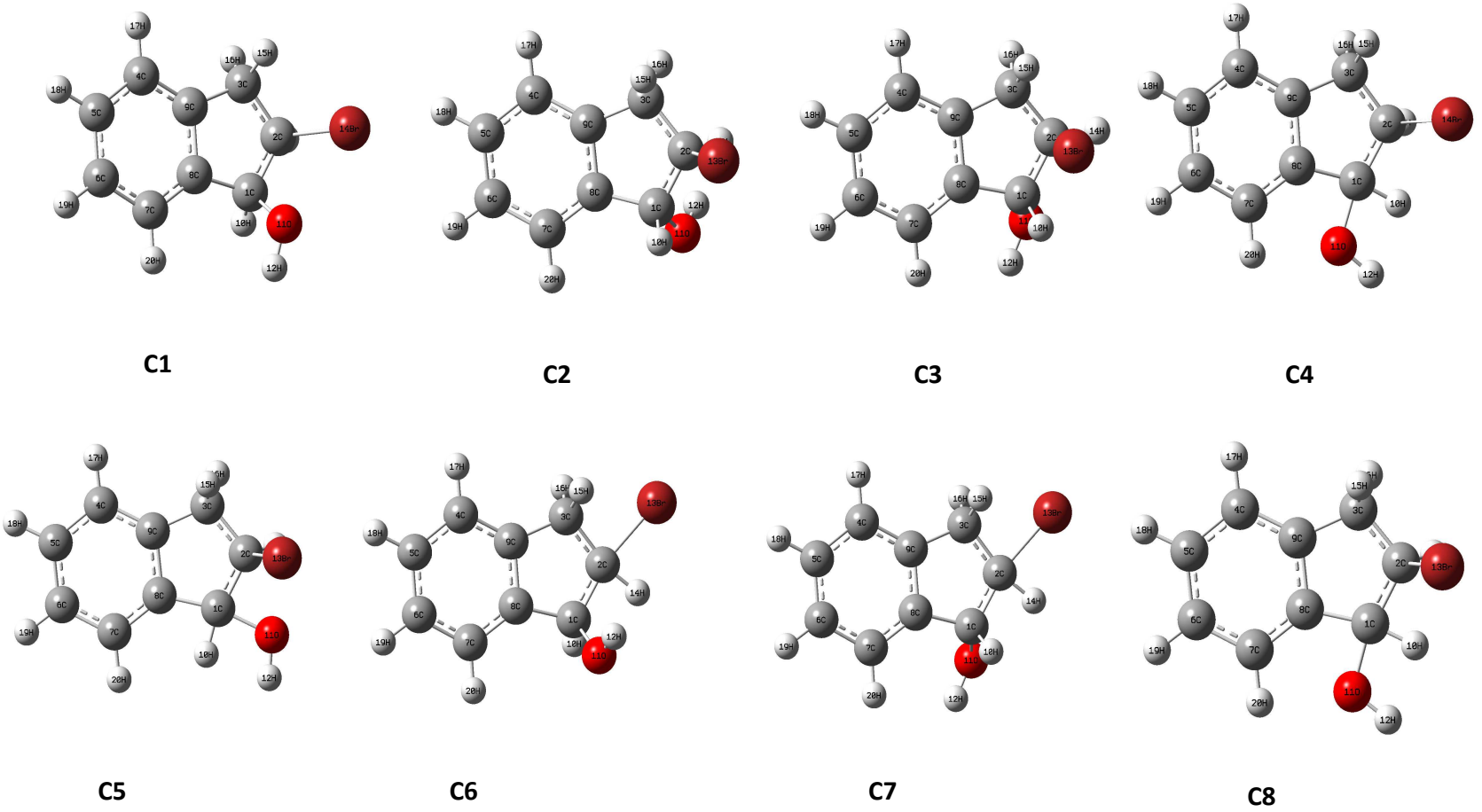

Fig 1 Various possible conformers of 2-bromo-1-indanol

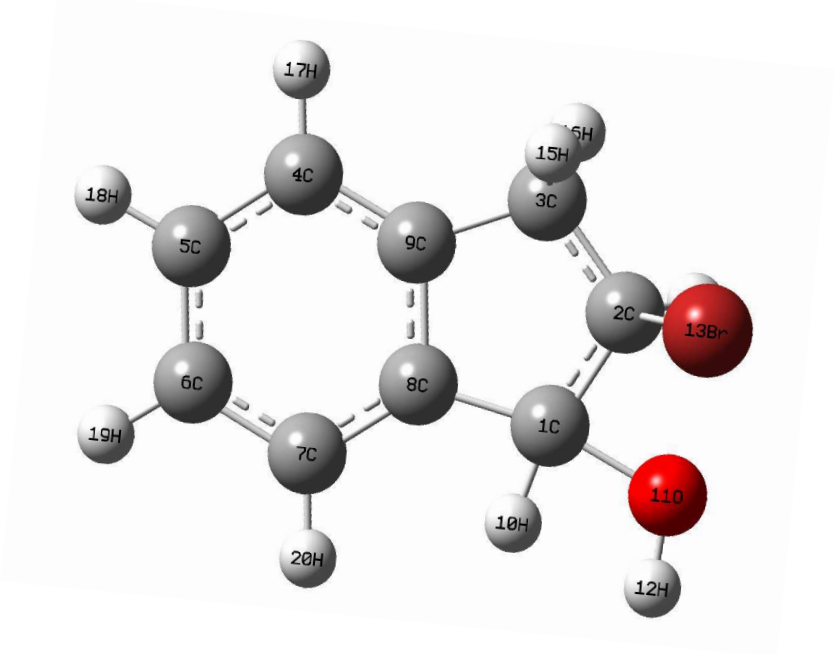

Fig 2 Optimized molecular structure of 2-bromo-1-indanol

Potential energy distribution

To check whether the chosen set of symmetric coordinates contribute maximum to the potential energy associated with the molecule, the PED has been carried out. The vibrational problem was set-up in terms of internal and symmetry coordinates. The geometrical parameters of the molecule were allowed to relax and all the calculations converged to an optimized geometry which corresponds to a true minimum, as revealed by the lack of imaginary values in the wavenumber calculations. The Cartesian representation of the theoretical force constants have been computed at the fully optimized geometry by assuming Cs point group symmetry.

Table 3 Definition of local symmetry co-ordinates of 2-bromo 1-Indanol

Sno	Symbol	Definition
1-10	CC	R1, R2, R3, R4, R5, R6, R7, R8, R9, R10
11-18	CH	t11, t12, t13, t14, t15, t16, t17, t18
19	CO	P19
20	CBr	Q20
21	OH	S21
22-24	bCC	(β22–β23+β24–β25+β26–β27+β28–β29+β30)/ √6
	βsym	(–β22–β23+2β24–β25–β26+2β27–β28–β29+2β30) / √12
	βasym	(β22–β23+β25–β26+β28–β29)/ 2
25-32	bCH	(σ31–σ32) / √2, (σ33–σ34) / √2, (σ35–σ36) / √2, (σ37–σ38) / √2, (σ39–σ40) / √2, (σ41–σ42) / √2, (σ43–σ44) / √2, (σ45–σ46) / √2
33	bCO	(α47–α48) / √2
34	bCBr	(ρ49–ρ50) / √2
35	bCOH	λ51
36	bHOH	α52
37	bHBr	α53
38-40	tRing	(ω54–ω55+ω56–ω57+ω58–ω59+ω60–ω61+ω62)/ √6
	tRing sym	(–ω54–ω55+2ω56–ω57–586+2ω59–ω60–ω61+ω62) / √12
	tRing asym	(ω54–ω55+ω57–ω58+ω60–ω61)/ 2
41-48	ωCH	τ63, τ64, τ65, τ66, τ67, τ68, τ69, τ70
49	ωCO	ω71
50	ωCOH	(τ72–τ73) / √2
51	ωCBr	τ74
52	ωHOH	ω75
53	ωHBr	ω76
54	ωHCH	ω77

The symmetry of the molecule was also helpful in making vibrational assignment. The transformation of force field, subsequent normal coordinate analysis and calculation of the PED were done on a PC with the MOLVIB program (version V7.0-G77) written by Tom Sundius [19, 20].

Vibrational analysis

The molecule 2BI belongs to C1 point group symmetry. The 54 normal modes of vibrations of 2BI are distributed among the symmetry species as Γvib = 37A'+17A". The A' and A" represent the in-plane and out-plane vibrations, respectively. All vibrations are active both in the infrared absorption and Raman scattering. The calculated IR and Raman intensities and normal mode descriptions are reported in Table 5. The FT-IR and FT-Raman spectra of 2BI at are shown in Fig. 3 and 4, respectively.

Table 4 Optimized geometrical parameters of 2-bromo 1-Indanol calculated at the HF / 6-31+G (d) and B3LYP / 6-31+G (d) levels of theory

Parameter	Bondlength		Parameter	Bondangle	
	HF	B3LYP		HF	B3LYP
C1–C2	1.53	1.54	C2–C1–C3	103.90	104.02
C1–C9	1.53	1.54	C2–C1–O11	113.87	114.14
C1–O11	1.39	1.41	C8–C1–O10	110.81	110.54
C1–H10	1.08	1.09	C8–C1–H11	108.95	109.03
C1–C8	1.50	1.50	O11–C1–H10	110.58	110.53
C2–H10	2.14	2.15	C2–C1–C8	103.53	103.99
C2–Br13	1.96	1.98	C1–C2–Br13	111.42	111.07
C2–H14	1.07	1.09	C1–C2–H14	110.89	110.91
C3–C4	1.38	1.39	C8–C2–H12	99.56	100.61
C3–C9	1.38	1.39	C3–C2–Br13	114.55	114.52
C3–H15	1.07	1.08	C3–C2–H14	112.58	113.17
C4–C5	1.39	1.40	H15–C3–H16	135.69	135.14
C4–H17	1.07	1.08	Br13–C2–H14	104.04	103.36
C5–C6	1.38	1.39	C4–C5–C9	118.70	118.76
C5–H18	1.07	1.08	C9–C3–H15	120.47	120.64
C6–C7	1.38	1.39	C9–C3–H16	120.81	120.58
C6–H19	1.07	1.08	C4–C9–C3	120.45	120.47
C7–C8	1.38	1.40	C9–C4–H17	119.78	119.73
C8–C9	1.51	1.51	C5–C4–H17	119.75	119.78
C3–H16	1.08	1.09	C4–C5–C6	120.57	120.56
C7–H20	1.08	1.09	C4–C5–H18	119.65	119.70
O11–H12	0.94	0.97	C6–C5–H18	119.77	119.72
H10–H12	2.86	2.86	C5–C6–C7	119.03	119.14
			C5–C6–H19	120.26	120.27
			C7–C6–H19	120.70	120.57
			C6–C7–C8	120.16	120.05
			C7–C8–C1	129.01	129.12
			C9–C8–C1	110.74	110.73
			C3–C9–C4	129.73	129.75
			C3–C9–C8	109.119	109.13
			C4–C9–C8	121.05	120.99
			C2–C1–C8	102.56	102.85
			C2–C1–H10	109.37	108.94
			C8–C1–H10	111.00	111.18
			C9–C3–H15	113.95	114.11
			H15–C3–H16	107.78	107.45
			C1–O11–H12	110.32	108.73
			C1–C2–Br13	81.20	81.97
			C2–C3–H16	112.08	112.21

O–H vibrations

The hydroxyl stretching vibrations are generally [21] observed in the region around 3500 cm $^{-1}$. The peak is broader and its intensity is higher than that of a free OH vibration, which indicates involvement in an intermolecular hydrogen bond. Hydrogen grouping undergo self-association and their spectra are accordingly very dependent on the state of the sample. Hydroxyl compounds in solid and pure liquid state normally exist as polymeric aggregates held together by hydrogen bonds that break up on dilution with non polar solvents first to trimers or dimers and finally, on large dilution to monomers. The highly hindered hydroxyl group displays a free O–H stretching wavenumber even in the pure state for (2BI) exhibits a free O–H stretching. Hydrogen bonding alters the wavenumbers of the

stretching and bending vibrations. The O–H stertching bonds move to lower wavenumbers usually with increased intensity and bond broadending in the hydrogen –bonded species. In the present study, the stretching vibrations of the hydroxy groups of (2BI) were observed at 3333 cm^{-1} in IR spectrum. The O–H in plane bending vibration is normally observed in the region from 1332 cm^{-1} in IR spectrum, the position of the band depending on the type of the hydyoxyl group [22].

As seen from the PED values shown in Table 5 the O–H in plane vibrations are strongly mixed with other vibrations. The O–H torsional vibration is very anharmonic; therefore, it is difficult to reproduce this wavenumber with a harmonic approach for (2BI). The wavenumber of this vibration was observed at 360 cm^{-1} in Raman spectrum.

C–O vibrations

The C–O stretching vibrations in the 2BI produce a strong band near 1360–1260 cm^{-1} and are sensitive to the nature of the subsituents bonded to the carbonyl carbon. Consequently, this provides valuable information in determining the nature of the hydroxyl compound. The characteristic response of 2BI in the infrared is associated with the stretchingvibration of the C–O–H system. Since the vibrational characteristics of this system would not be expected to differ greatly from the C–C–C system, it is not surprising to find that response to C–O–C vibrations involving oxygen atoms results in greater dipole moment changes than those involving carbon atoms. Both these bands involve some interaction between C–O stretching and inplane C–O–H bending. The most important contribution to the C–O stretching mode was at 1205 cm^{-1} for 2BI [23].

C–H vibrations

For simplicity, modes of vibrations of aromatic compounds are considered as separate C−H or ring C−C vibrations. However, as with any complex molecules, vibrational interactions occur and these levels only indicate the predominant vibration. Substituted benzenes have large number of sensitive bands, that is, bands whose position is significantly affected by the mass and electronic properties, mesomeric or inductive of the substituents. Accordingly to the literature [24, 25], in infrared spectra most mono nuclear and poly nuclear aromatic compounds have three or four peaks in the region 3000–3100 cm^{-1} these are due to the stretching vibrations of the ring CH bands. Accordingly, in the present study, the FT-IR and FT- Raman bands identified at 3092, 3072, and 2979 cm^{-1} are assigned to C–H stretching vibrations of 2BI are in good agreement with calculated values by B3LYP/6-31+G (d) 3175, 3154 and 3059 cm^{-1}. The FT-IR band at 1144, 1611, 1509, 1277 cm^{-1} and the FT-Raman band at 1560, 1263 cm^{-1} are assigned to C–H in-plane bending vibration of 2BI. The C–H out-of-plane bending vibrations of the title compound are well indentified at 1022, 814 cm^{-1} in the FT-IR and 1105, 1013, 987, 940, 526 cm^{-1} in the FT-Raman spectra are found to be well within their characteristic region.

C–C vibrations

The ring C=C and C–C stretching vibrations, known as semicircle stretching usually occurs in the region 1400–1625 cm^{-1} [26, 27]. Hence in the present investigation, the FT-IR bands indentified at 1811, 1699, 1455, 1120, 890 cm^{-1} and the FT-Raman bands at 1461, 1320, 1274, 1217 and 881 cm^{-1} are assigned to C–C stretching vibrations of 2BI. The band ascribed at 1122, 737 cm^{-1} in FT-IR and 615, 335, 743, 150, 120 cm^{-1} in FT-Raman spectra has been designated to CC in-plane and out-of-plane bending mode. The calculated bending modes found at 1152, 631, 344, 757, 154 and 122 cm^{-1} in B3LYP/6-31+G (d) are assigned to C–C in-plane and out-of-plane bending vibrations, respectively.

C–Br vibration

The assignment of C–Br stretching and deformational vibrations has been made on the basis of the calculated PED and by comparison with similar molecules-p-bromophenol [28] and the halogen substituted benzene derivatives [29]. Mooney [30, 31] assigned vibrations of C–X group {X=Cl, Br, I} in the frequency range of 1129 – 480 cm^{-1}. The medium FT-Raman band at 551 cm^{-1} corresponds to C–Br stretching mode. The theoretical wavenumber of this band at 566 cm^{-1} coincident well with the experimental, and the calculated PED confirms this assignment.. The C–Br out-of-plane bending and in-plane bending vibrations are assigned to the IR and Raman bands at 229 and 400, 409 cm^{-1}, respectively. This is in assignment with the literature data [28-31].

Table 5 Vibrational wave numbers obtained for 2BI at B3LYP/6-31+G (d) and HF/ 6-31+G (d) (wavenumber(cm^{-1}); IR intensities (Km mol^{-1}); Raman intensities (Å amu^{-1})

species	Observed frequency		Calculated frequency		Scaled frequency		PED assignments
	IR	Raman	HF	DFT	HF	DFT	
1	3333(vs)		4093	3734	3911	3422	υ OH(100)
2	3092(vs)		3389	3208	3238	3175	υ CH(99)
3		3072(s)	3378	3198	3228	3154	υ CH(98)
4		3052(vs)	3365	3188	3215	3133	υ CH(98)
5	3047(ms)		3354	3179	3205	3128	υ CH(98)
6	2979(ms)		3304	3109	3157	3059	υ CH(95)
7		2923(ms)	3268	3100	3123	3001	CH_2 ass(72)
8	2911(s)		3231	3044	3087	2989	CH_2 ss(78)
9	2866(ms)	2871(ms)	3214	3036	3071	2943	υ CH(94)
10	1811(ms)		1807	1659	1807	1859	υ CC(80)+ υCH(12)
11	1699(w)		1773	1631	1773	1744	υ CC(82)+ υ CH(10)
12	1644(w)		1644	1518	1644	1688	δ CH(68)+δ CO(23)
13		1615(ms)	1635	1508	1635	1658	CH_2 sciss(55)+υCC(18)+υCH(10)
14	1611(w)		1624	1502	1624	1654	δ CH(68)+ υ CC(13)+ CH_2 sciss(10)
15		1560(s)	1570	1429	1570	1602	δ CH(78)+υCC(19)
16	1509(ms)		1509	1377	1509	1549	δ CH(75) +υ CC(20)
17	1455(s)	1461(ms)	1461	1358	1461	1494	υ CC(72)+ δ OH(14)+ δ CH(11)
18		1425(ms)	1428	1334	1428	1463	CH_2 rock(54)+δCH(20)+υCC(12)
19	1332(vs)		1397	1299	1397	1368	δ OH(68)+δCO(22)
20		1320(m)	1364	1273	1364	1355	υ CC(62)+δ CO(24)
21	1296(s)		1348	1249	1348	1331	υ CC(60)+ δ CH(14)+δCBr(12)
22		1287(w)	1330	1238	1330	1321	Ring breathing(62)
23	1277(s)		1321	1223	1321	1311	δ CH(64)+ υ CH(20)+δCCC(10)
24		1274(m)	1284	1194	1284	1308	υ CC(63)+ υ CH(20)
25		1263(m)	1276	1190	1276	1297	δ CH(59)+ υ CO(23)+δCO(11)
26	1222(s)		1234	1169	1234	1255	CH_2 twist(68)+γCC(18)
27		1217(s)	1216	1127	1216	1249	υ CCC(62)+ υ Br(18)+δCC(11)
28		1205(m)	1200	1101	1200	1237	υ CO(75)+δ CH(15)
29		1153(m)	1153	1054	1153	1184	CH_2 wag(58)+γCO(21)+γCH(10)
30	1122(s)		1125	1050	1125	1152	δ CC(68)+ δ CO(18)+δCH(10)
31	1120(s)		1121	1017	1121	1150	υ CCC(73)+ CH_2 sciss(10)
32		1102(m)	1110	994	1110	1131	γ CH(69)+γ CC(13)
33	1022(w)	1013(vs)	1073	951	1073	1049	γ CH(76)+ γ CC(15)
34		987(m)	992	905	992	1013	γ CH(83)+ γ OH(12)
35		940(m)	970	881	970	965	γ CH(88)+γ Br(10)
36	890(ms)		936	871	936	914	υ CCC(68)+ υ CH(20)
37		881(m)	881	823	881	905	υ CCC(62)+ δ CC(18)
38	857(vs)	846(m)	852	777	852	880	γ CC(76)+ γ CH(20)
39	814(s)		830	756	830	836	γ CH(68)+ γ CO(15)+γCC(12)
40	737(vs)	743(s)	761	705	761	757	γ CC(76)+ CH_2 rock(12)
41		667(vs)	695	647	695	685	δ CC(69)+ δ OH(14)+δCH(11)
42		615(ms)	644	600	644	631	δ CCC(73)+ δ CH(14)
43		551(ms)	556	512	556	566	υ Br(83)+ υ CC(12)
44		526(s)	538	500	538	540	γ CH(85)+ γ CC(10)
45	487(ms)		500	465	500	500	δ CO(58)+ CH_2 sym(18)+δCCC(12)
46		461(ms)	464	429	464	473	γ CO(60)+ γ OH(22)
47	400(ms)	409(ms)	418	385	418	411	δ Br(63)+ δ CC(15)
48		360(w)	369	355	369	370	γ OH(75)+ γ CC(20)
49		335(w)	335	307	335	344	δ CCC(67)+ CH_2 twist(17)
50		267(w)	265	243	265	274	γ CC(66)+ γ CH(20)
51		229(w)	236	217	236	235	γ Br(55)+ γ CH(14)+γCCC(12)
52		150(w)	154	139	154	154	γ CCC(42)+γ OH(17)+γCCC(10)
53		120(w)	122	111	122	123	γ CCC(66)+ γ CH(16)
54			74	64	74	0	Butterfly(98)

υ – stretching, δ – in-plane, γ – out-of-plane, w – weak, m – medium, s – strong, vs – verystrong, vw – veryweak

Mulliken population analysis

Mulliken atomic charge calculation has an important role in the application of quantum chemical calculation to molecular system because of atomic charge effect dipole moment, molecular polarizability, electronic structure and more a lot of properties of molecular system. The bonding capability of a molecule depends on the electronic charge on the chelating atoms. The atomic charge values were obtained by the Mulliken population analysis [32]. The calculated Mulliken charge values are listed in Table 6. The charge changes with basis set presumably occurs due to

polarization. For example, the charge of Br (13) atom is–0.098346 e for B3LYP/ 6-31+G (d) and – 0.737631e for HF/6-31+G (d). The charge distribution of bromine atom is increasing trend in HF and B3LYP. Considering all the methods and basis set used in the atomic charge calculation, the carbon atoms exhibit a substantial negative charge, which are donor atom. Hydrogen atom exhibits a positive charge, which is an acceptor atom. The C–Br bond length of 2BI is closer with normal C–Br bond length (ca. 1.98 Å) due to the attraction effect between C–Br atoms.

Table 6 Calculated values of Mullikan atomic charges

S. No	Atom	Charges	
		DFT	HF
1	C1	0.91366	0.837518
2	C2	−1.977024	−1.968375
3	C3	−0.147159	−0.329044
4	C4	−0.015733	−0.194346
5	C5	−0.006074	−0.249135
6	C6	0.053633	−0.136538
7	C7	−0.250561	−0.012813
8	C8	0.760288	1.069013
9	C9	−0.823047	−0.846594
10	O11	−0.382593	−0.492112
11	H10	0.431464	0.487288
12	H12	0.169290	0.220553
13	Br13	−0.098346	−0.751631
14	H14	0.274621	0.296566
15	H15	0.190053	0.251430
16	H16	0.178024	0.233537
17	H17	0.174631	0.230557
18	H18	0.715272	0.232883
19	H19	0.225516	0.221618
20	H20	0.276379	0.281125

NBO analysis

NBO analysis is proved to be an effective tool for chemical interpretation of hyper conjugative interaction and electron density transfer (EDT) from filled lone electron pairs of the n (Y) of the "Lewis base" Y into the unfilled antibond σ* (X–H) of the "Lewis acid" x–H in X–H…….Y hydrogen bonding systems [33]. Also, in order to obtain structure of molecule 2BI, the main natural orbital interactions were analyzed with the NBO 3.0 program [34]. The lowering of orbital energy due to the interaction between the doubly occupied orbital and the unoccupied ones is a very convenient guide to interpret the molecular structure. In energetic terms, hyperconjucation is an important effect [35, 36] in which an occupied Lewis-type natural bond orbitals stabilized by overlapping with a non Lewis-type orbital (either one-center Rydberg's or two-center antibondig NBO). This electron delocalization can be described as a charge transfer from a Lewis valence orbital (donor), with a decreasing of its occupancy, to a non-Lewis orbital (acceptor). Several other types of valance data, such as directionality, hybridization and partial charges were analyzed in Table 7, the output of NBO analysis.

Table 7 NBO results showing the formation of Lewis and non Lewis orbital's by valence hybrids corresponding to the intermolecular C-H…O hydrogen bonding of E122.

BondA–B	Occupancy	ED_A	ED_B	NBO%	S%	P%
BD(C1–C2)	1.91662	53.33	46.67	$0.7302sp^{1.58}+0.6832sp^{2.54}$	38.66, 28.23	61.26,71.65
BD*(C1–C2)	0.07739	46.67	53.33	$0.6832sp^{1.58}–0.7302sp^{2.54}$	38.66, 28.23	61.26,71.65
BD(C1–O11)	1.93576	32.74	67.26	$0.5722sp^{17.00}+0.8201sp^{2.68}$	5.54, 27.12	94.18, 72.76
BD*(C1–O11)	0.08666	67.26	32.74	$0.8201sp^{17.00}–0.5722sp^{2.68}$	5.54, 27.12	94.18, 72.76
BD(C2–Br13)	1.97029	49.05	50.95	$0.7003sp^{6.86}+0.7138sp^{6.73}$	12.71, 12.90	87.19, 86.88
BD*(C2–Br13)	0.10266	50.95	49.05	$0.7138sp^{6.86}–0.7003sp^{6.73}$	12.71, 12.90	87.19, 86.88
BD(C2–H14)	1.91199	67.48	32.52	$0.8214sp^{2.17}+0.5703sp^{0.00}$	31.56, 100	68.37
BD*(C2–H14)	0.10266	32.52	67.48	$0.5703sp^{2.17}–0.8214sp^{0.00}$	31.56, 100	68.37
BD(C3–C9)	1.97432	48.36	51.64	$0.6954sp^{1.90}+0.7186sp^{1.61}$	34.52, 38.25	65.43, 61.72
BD*(C3–C9)	0.02147	51.64	48.36	$0.7186sp^{1.90}–0.6954sp^{1.61}$	34.52, 38.25	65.43, 61.72
BD(C3–H15)	1.95197	62.69	37.31	$0.7918sp^{4.02}+0.6108sp^{0.00}$	19.93, 100	80.01
BD*(C3–H15)	0.02622	37.31	62.69	$0.6108\ sp^{4.02}–0.7918\ sp^{0.00}$	19.93, 100	80.01
BD(C3–H16)	1.93300	64.42	35.58	$0.8026sp^{2.83}+0.5965sp^{0.00}$	26.12, 100	73.83
BD*(C3–H16)	0.01903	35.58	64.42	$0.5965sp^{2.83}–0.8026sp^{0.00}$	26.12, 100	73.83
LP O11	1.93736			$sp^{0.72}$	58.16	41.79
LP Br13	1.99531			$Sp^{0.15}$	87.02	12.97

Table 8 The second order perturbation energies $E^{(2)}$ (kal/mol) corresponding to the most important charge transfer interactions (donor - acceptor) in the compounds studied by B3LYP/6-31+G (d, p) method

Sno	Bond	Accepter	E(2)	E(j)-E(i)	F(I,j)
1	BD C1–C2	BD* C1–C2	1.21	1.14	0.33
2	BD C1–C2	BD* C2–Br13	0.70	0.77	0.021
3	BD C1–C2	BD* O11–H12	15.82	1.03	0.114
4	BD C1–C8	BD* C1–O11	0.95	0.85	0.026
5	BD C1–C8	BD* C2–C3	0.95	1.06	0.030
6	BD C1–O11	BD* C1–O11	2.49	0.92	0.043
7	BD C1–O11	BD* C2–H14	3.46	1.21	0.058
8	BD C1–H10	BD* C3–H16	0.80	0.94	0.025
9	BD C1–H10	BD* O11–H12	0.68	0.84	0.021
10	BD C2–C3	BD* C1–C2	1.78	1.12	0.040
11	BD C2–Br13	BD* C1–C2	0.81	1.65	0.026
12	BD C2–H14	BD* O11–H12	9.65	0.86	0.082
13	BD O11–H12	BD* C1–O11	1.55	0.91	0.034
14	BD O11–H12	BD* C2–H14	1.22	1.21	0.034
15	LP O11	BD* C1–C2	1.71	1.13	0.039
16	LP Br13	BD* C2–H14	0.52	1.41	0.024
17	LP(2) O11	BD* O11–H12	2.41	0.02	0.044

Table 8 gives the second-order perturbation energy, E_{ij} (2) corresponding to the interactions and the overlap integral of each orbital pair. From the table very strong hyper conjugative interaction is observed between the π type orbital containing the lone electron pair of O10 and the neighbor C1−C2 antibonding orbital of the benzene ring. The π electrons of C2−H14 towards the n (LP Br13) orbital and the overlap of donor and acceptor orbitals are well known. This interaction is responsible for a prounced of the lone pair orbital occupancy. The hyper conjugation between O9 and the benzene ring defines the common molecular feature of this type of molecules. An important contribution for the molecular stabilization energy is further given by O10 through the overlap of its $sp^{0.15}$ lone pair n (LP Br13) with the π* (C2−H14) orbital and shows the hyper conjugation interaction.

HOMO–LUMO energy

In principle, there are several ways to calculate the excitation energies. The simplest one involves the difference between the highest occupied molecular orbital (HOMO) and the lowest unoccupied molecular orbital (LUMO) of a neutral system, and is a key parameter determining molecular properties. The frozen orbital approximation and the ground state properties are used to calculate the excitation values. This method is very practical, particularly for calculating large system [37**].** Rigorously, the density functional methods (which are based on Hohenberg and Kohn theorem [38] are designed to yield total energies. However, the orbitals in this case (Kohn-Sham orbitals [39]) are not electronic orbitals but mathematical arrangements and their Eigen values are not directly related to the electronic excitation energies. Nevertheless, it is often a good approximation to neglect these formal inconsistencies and consider them as electronic orbitals and orbital energies, as they are in the HF framework [40]. The Eigen values of LUMO and HOMO and their energy gap reflect the chemical activity of the molecule. The HOMO energies, the LUMO energies and the energy gap for 2BI molecules have been calculated using B3LYP level with 6-31+G (d) basis set. An electronic system with a larger HOMO–LUMO gap should be less reactive than one having a smaller gap [41]. The 3D plots of the HOMO and LUMO for the 2BI is shown in Fig. 5. In 2BI the highest occupied molecular orbitals are localized mainly on all atoms, the lowest unoccupied molecular orbitals are also mainly on the carbon atoms having single bonds only in the ring, which also indicate that, the electron density transfer from n with the π* orbitals, so electronic transitions from the HOMO to the LUMO are mainly derived from the electronic transitions of n→ π*. From the result the

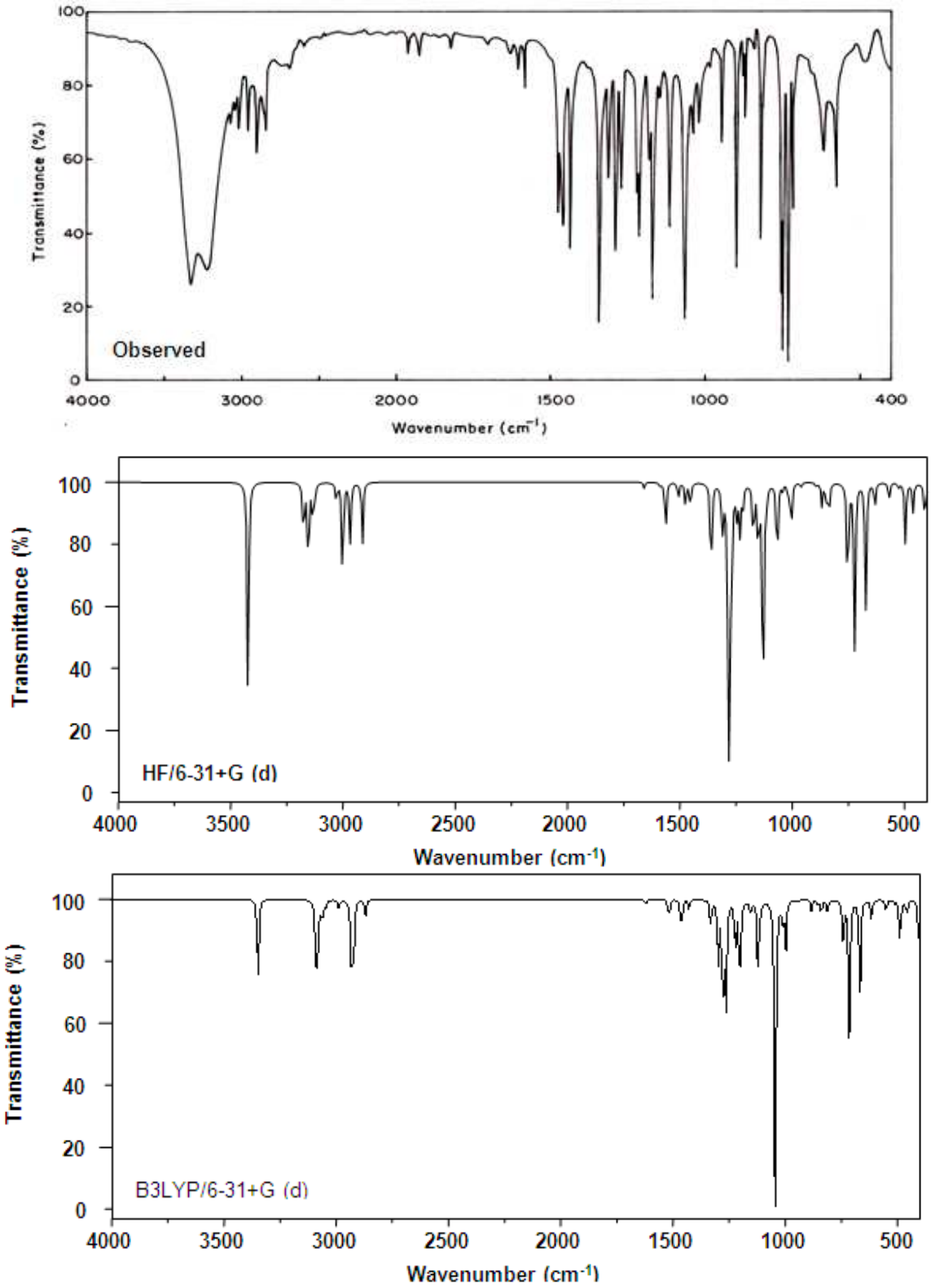

Fig 3 Observed and simulated FT-IR spectra of 2-bromo-1-indanol

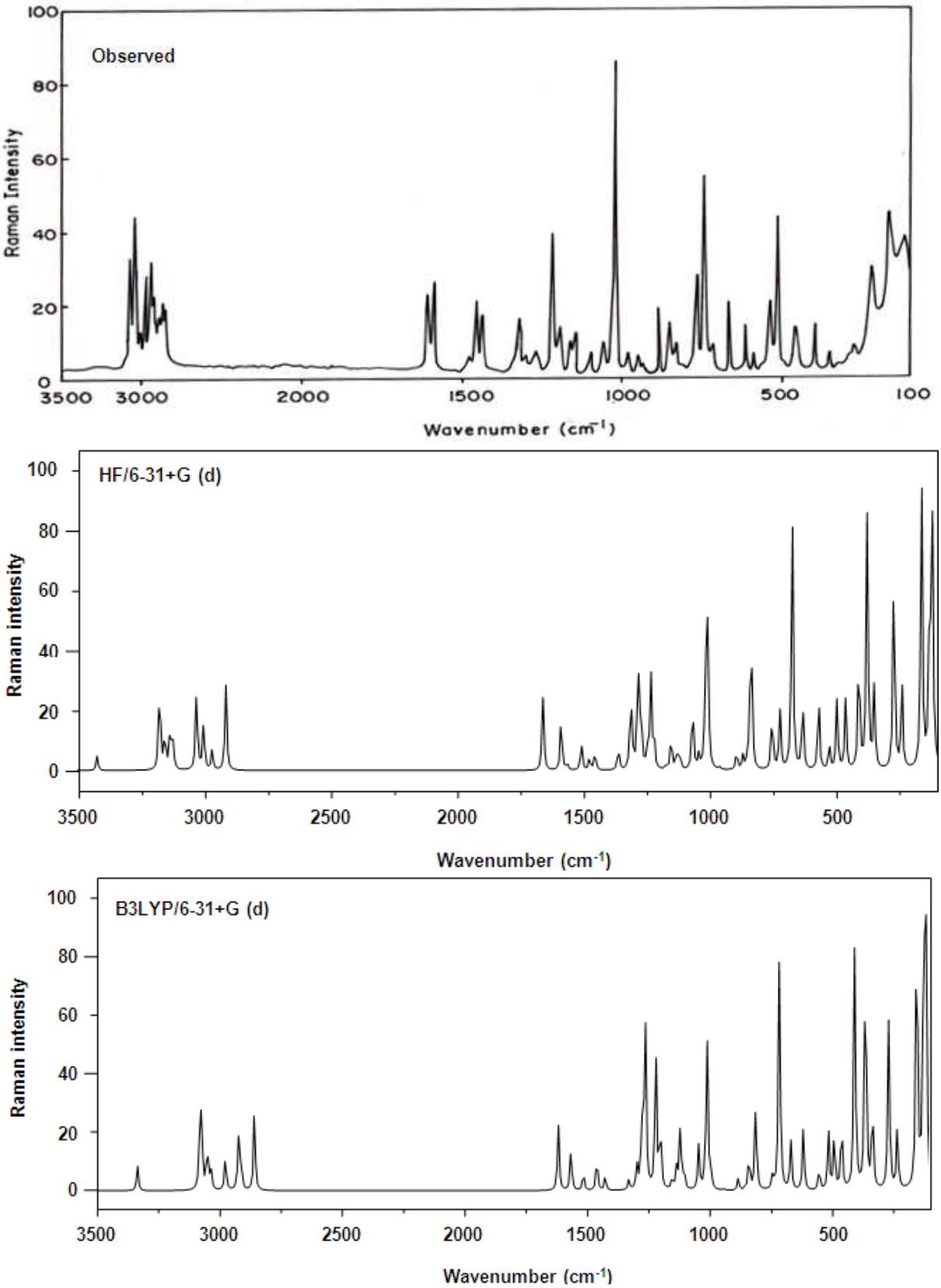

Fig 4 Observed and simulated FT-Raman spectra of 2-bromo-1-indanol

HOMO energy = –0.20119 a.u
LUMO energy = – 0.04402 a.u
The energy gap = – 0.24521 a.u

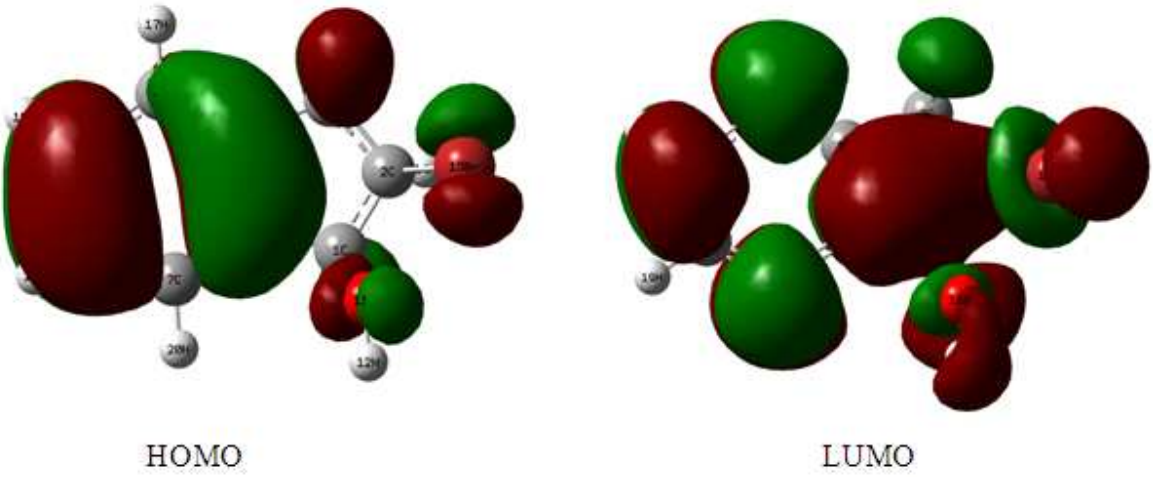

Fig. 5 The atomic orbital compositions of the frontier molecular orbital for 2-bromo-1-indanol

Electrostatic potential

Electrostatic potential (ESP) at a point in space around a molecule gives Information about the net electrostatic effect produced at that point by total charge distribution (electron+ proton) of the molecule and correlates with dipole moments, electro negativity, partial charges and chemical reactivity of the molecules. It provides a visual method to understand the relative polarity of the molecule. An electron density isosurface mapped with electrostatic potential surface depicts the size, shape, charge density and site of chemical reactivity of the molecules.

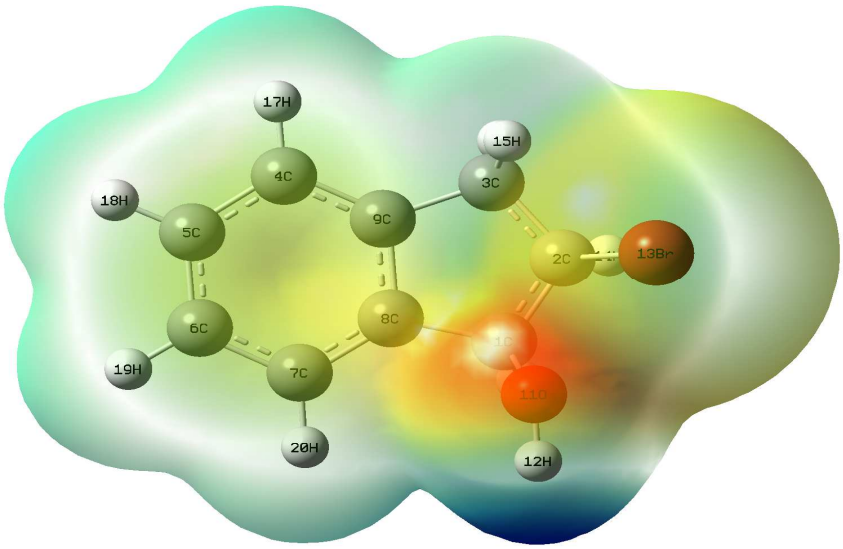

Fig. 6 Electrostatic potential map of 2-bromo-1-indanol

The electrostatic potential at the surface are represented by different colors; red represents regions of most electronegative, blue represents regions of the most positive electrostatic potential and green represents region of zero potential. Potential decreases in the order red < orange < yellow <green < blue. Such mapped electrostatic

potential surface have been plotted for title molecule in B3LYP/6-31+G (d) basis sets using the computer software Gauss view. Projections of these surfaces along the molecular plane and a perpendicular plane are given in Fig. 6. The hydroxyl group of H atom posses more positive in Nucleophilic region, lone pair of oxygen atom posses more electro negative. This figure provides a visual representation of the chemically active sites and comparative reactivity of atoms [42].

Thermodynamic properties

The total energy of a molecule is the sum of translational, rotational, vibrational and electronic energies, i.e., $E = E_t + E_r + E_v + E_e$. The statistical thermo chemical analysis of 2BI is carried out considering the molecule to be at room temperature of 298.15 K and one atmospheric pressure. The thermodynamic parameters, like rotational constant, zero point vibrational energy (ZPVE) of the molecule by DFT method with B3LYP are presented in Table 1 for C5 conformer. On the basis of vibrational analysis and statistical thermodynamics, the standard thermodynamic functions: heat capacity ($C^0_{p,m}$), entropy (S^0_m), and enthalpy (H^0_m) were obtained and listed in Table 9. As is evident from Table 9, all the values of $C^0_{p,m}$, S^0_m, and H^0_m increases with the increase of temperature from 100.0K to700.0K, which is attributed to the enhancement of the molecular vibration while the temperature increases because at a constant pressure (db = 1 atm) values of $C^0_{p,m}$, S^0_m, and H^0_m are equal to the quantity of temperature [43]. The correlations between these thermodynamic properties and temperatures T are shown in Figs.7, 8 and 9. Notice: all the thermodynamic calculations were done in gas phase and they could not be used in solution. Scale factors have been recommended [44] for an accurate prediction in determining the zero-point vibration energies, heat capacities, entropies, enthalpies and Gibbs-free energies.

Table 9 Thermodynamic parameters of 2-bromo1-Indanol.

Temp. (K)	$C^0_{p,m}$ (cal mol^{-1} K^{-1})		S^0_m (cal mol^{-1} K^{-1})		ΔH^0_m (kcal mol^{-1})	
	HF	B3LYP	HF	B3LYP	HF	B3LYP
100	2.99	3.67	4.58	8.07	1.60	4.40
200	10.55	11.57	17.19	24.16	6.64	12.60
300	23.03	24.22	38.70	49.10	15.67	24.89
400	40.71	41.96	69.72	83.46	29.00	41.50
500	63.61	64.82	110.45	127.46	46.84	62.63
600	91.48	92.60	160.78	180.97	69.30	88.37
700	123.96	124.97	220.37	243.71	96.40	118.74

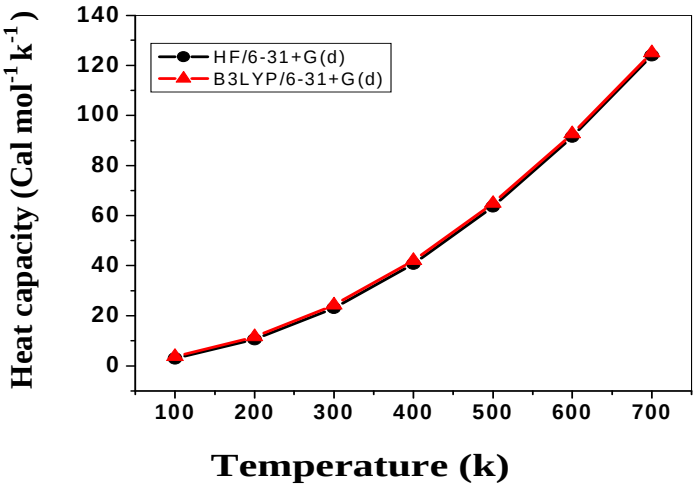

Fig 7 Correlation graph of heat capacity and temperature for 2-bromo-1-indanol

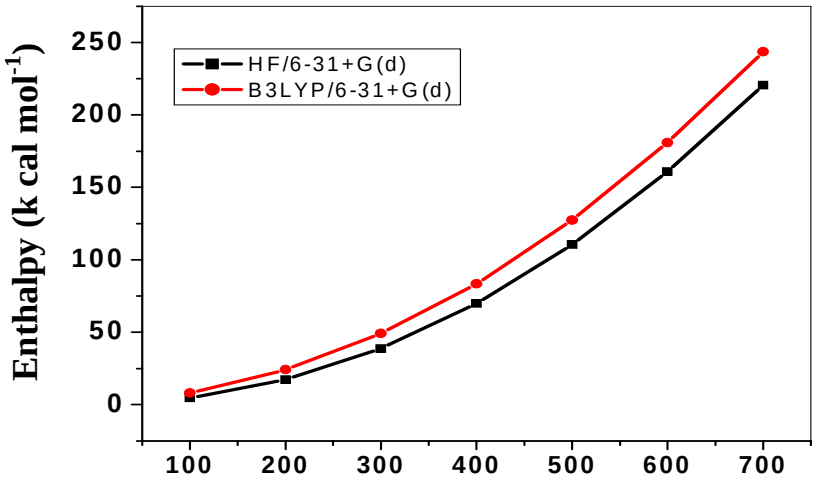

Fig 8 Correlation graph of enthalpy and temperature for 2-bromo-1-indanol

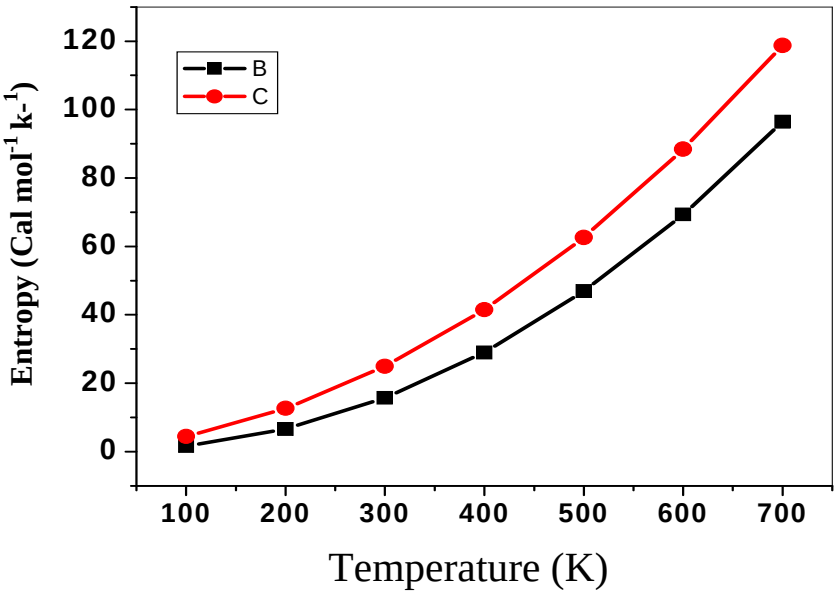

Fig 9 Correlation graph of entropy and temperature for 2-bromo-1-indanol

CONCLUSION

Based on the density functional theory calculations a complete vibrational analysis has been done by FT-IR and FT-Raman spectroscopic techniques. The vibrational frequencies analysis by B3LYP/6-31+G (d) method agrees satisfactorily with experimental results, compared to HF/6-31+G (d) method. The geometry optimization exposes the planarity of 2BI molecule. The Mulliken charge analysis explains the possibilities of hydrogen bonding. The pronounced decrease of the lone pair orbital occupancy and the molecular stabilization energy show the hyperconjucative interaction from the NBO analysis. The scaled frequencies of the FT-IR and Raman spectra are well consistent with that of the experimental spectra. The strengthening and polarization band increase in IR due to the degree of conjugation, and the O–H bending character reveals the intermolecular hydrogen bonding interactions. The HOMO–LUMO energy has also been occupied. The ESP gives the visual representation of the chemically

active sites and comparative reactivity of atoms. Thermodynamic properties in the range from 100 K to 700 K are obtained. The gradients of Cp,m, Sm, Hm, and vibrational intensity increases with increase of temperature.

REFERENCES

[1] T Pena Ruiz, PhD. Thesis, University of Jane, Jane, Spain, **2003**(ISBN 84-8439-196-5).
[2] K Lee, SM Resnik, DT Gibson, *Appl. Environ*. **1997,** 63, 2067−2070.
[3] DE Stafford, KS Yanagimaci, G Stephanopoulos, in: Th. Scheper (Ed.). Advances in Biochemical Engineering/ biotechnology, vol. 73. Springer, Berlin/Heidelberg, **2001**.
[4] L Bardet, G Fleury, R Granger, C Sablayrolles, *J. Mol. Struct*. **1969**, 3, 141−150.
[5] G Rauhut, P Pulay, *J. Phys. Chem*. **1995**, 99, 3093−3100.
[6] G Rauhut, P Pulay, *J. Am. Chem. Soc*. **1995**, 117, 4167−4172.
[7] P Pulay, G Fogarasi, G Ponger, JE Boggs, A Vargha, *J. Am. Chem. Soc*.**1983**, 101, 7037−7043.
[8] P Pulay, *J.Mol. Struct*. **1995**, 347, 293−308.
[9] J Frisch, GW Trucks, HB Schlegel, GE Scuseria, et. al. Gauss 09, Rev A,Vol.11.4 Gaussian Inc.,Pitts burgh,PA **2009**.
[10] AD Becke, *J. Chem. Phys*. **1993**, 98, 5648–5652.
[11] C Lee, W Yang, RG Parr, *Phys. Rev*. **1998**, 1377, 785–789.
[12] MJ Frisch, AB. Nielsm, AJ Holder, Gaussview User manual Gaussian Pitsburgh, **2008**.
[13] AE Reed, F Weinhold, *J. Chem. Phys.***1985,** 83, 1736–1740
[14] M Snehalatha, C Ravi Kumar, I Hubert Joe, VS Jaya Kumar, *J. Raman Spectrosc* **2009**, 40, 1121–1126.
[15] I Hubert Joe, I Kostova, C Ravi Kumar, M Amalanathan, SC Pinzaru, *J. Raman Spectrosc*. **2009**, 40, 1033–1038.
[16] AE Ledesma, J Zinczuk, A Ben Altabef, JJ Lopez Gonzalez, SA Brandan, *J. Raman Spectrosc*. **2009**, 40, 1004–1010.
[17] J Chocholousova, V Vladimir Spirko, P Hobza, *Phys. Chem. Chem. Phys*, **2004**, 6, 37–41.
[18] P Puiay, G Fogarasi, F Pong, JE Boggs, *J. Am. Chem. Soc.* **1979**, 101, 2550–2560.
[19] T Sundius, MOLVIB A Program for harmonic force field calculations QCPE program, No 604 1991.
[20] T Sundius, *Vib Spectrosc*,**2002**, 29, 89−95.
[21] B Smith, Infrared Spectral Interpretation, a Systematic Approach CRC Washington DC, **1999**.
[22] J Mohan, Organic Spectroscopy – Principles and application (2nd edn). Narosa Publishing House, New Delhi **2001**.
[23] M Silverstein, G Clayton, Bassler, C Morrill, Spectrometric identification of organic compounds, Wiley, New York, **1981**.
[24] S. Ramachandran, G. Velraj, *J. Chem. Pharm. Res*., **2012**, 4(12),5126−5138.
[25] M Murugan, V. Balachandran, M Karnan, *J. Chem. Pharm. Res*., **2012**, 4(7), 3400−3413.
[26] V Krishnakumar, R John Xavier, *Indian J. Pure Appl. Phys*. **2003**, 41, 95−98.
[27] K Furic, V Mohacek, M Bonifacic, I Stefanic, *J. Mol. Struct.* **1992**, 267, 39−44.
[28] W Zierkiewicz, D Michalska, Th Zeegers- Huyskens, *J. Phys. Chem. A.* **2000**, 104,11685−11692.
[29] G Varasanyi, Vibrational Spectra of Benzene Derivatives Academic Press New York, **1969**.
[30] EF Mooney *Spectrochim. Acta* **1964**, 20, 1021−1032.
[31] EF Mooney *Spectrochim. Acta* **1963,** 19, 877−887.
[32] RS Mulliken, *J. Chem. Phys.* **1955**, 23, 1833–1840.
[33] F Weinhold, C Landis, Valency and Bonding: A Natural Bond Orbital Donor-Acceptor Perspective, Cambridge University Press, Cambridge, **2005**.
[34] GA Jaffrey, An Introduction to Hydrogen Bonding, Oxford University Press: USA, **1997**.
[35] N Sundaraganesan, B Dominic Joshua, C Meganathan, R Meenashi, JP Cornad, *Spectrochim. Acta*. **2008**, 70, 376–383.
[36] LJ Bellamy, The Infrared Spectra of Complex of molecules, Vols. 1and 2, Chapmann and Hall, London, **1975**.
[37] LA Curtiss, PC Reghavachari, *J. Chem. Phys*.**1998**, 42, 117–122.
[38] P Hohenberg, W Kohn, *Phys. Rev. B* **1964**, 136, 864–871.
[39] W Kohn, LP Sham, *Phys. Rev. A* **1965**, 140, 1133–1138.
[40] M Springborg, in M. Springborg (Ed.), Density- Functional Method in Chemistry and Materials Science, John Wiley and Sons, Chichester, **1997**, p 207.
[41] R Kurtaran, S Odabasioglu, A Azizoglu, H Kara, O Atakol, *Polyhedron* **2007**, 26, 5069–5074.

[42] VP Gupta, A Sharma, V Virdi, VJ Ram, *Spectrochim. Acta*, **2006**, 64, 57–67.
[43]F Bopp, J Meixner, J Kestin, Thermodynamics and Statistical Mechanics, 5th ed., Academic Press Inc. (London) Ltd., New York, **1967**.
[44]G Varsanyi, P Sohar, *Acta Chim. Acad. Sci. Hung*. **1972**, 74, 315-333.